

Gap Effect on Flight Performance and Longitudinal Stability of Biplane Micro Air Vehicles

¹Muhammad Usman, ²Adnan Maqsood, ³Sundas R. Mulkana and ⁴Rizwan Riaz

Research Centre for Modeling & Simulation, National University of Sciences & Technology, Islamabad, Pakistan

Email: sheikh.babu@gmail.com, adnan@rcms.nust.edu.pk, smulkana.msse16@rcms.nust.edu.pk, and

rizwan@rcms.nust.edu.pk

Abstract— Comparative study on flight performance and longitudinal stability of biplanes with gap variation and monoplane Micro Air Vehicles (MAVs) are presented in this paper. The aerodynamic modeling is based on the experimental data collected at low Reynolds Number (~150,000) in a low-speed wind tunnel. A rigid flat plate with an aspect ratio of one and three different planform shapes (Zimmerman, inverse Zimmerman and Elliptical) are used to study the effect of gap between two wings on the flight performance characteristics. The trim states across a velocity spectrum of 5 and 15 m/s are evaluated using a nonlinear constrained optimization scheme based on hybrid Sequential Quadratic Programming (SQP) and quasi-Newton methods. The stability of these trim points is assessed numerically using Runge-Kutta methods. There is an evidence of emergence of Limit-Cycle Oscillations (LCO) at high angle of attack. The onset and amplitude of LCOs is earlier and larger for biplanes than monoplanes.

Index Terms— biplane, micro air vehicles, flight performance, trim point optimization, stability analysis

I. INTRODUCTION

Unmanned Air Vehicles (UAVs) are gaining importance round the globe with a plethora of advantages encompassing civilian and military roles. UAVs are becoming the first choice for non-lethal and lethal operations by military commanders. In civilian roles, they are gaining importance for versatile missions with a growing job market [1]. Successful utilization of UAVs has been demonstrated in Intelligence, Surveillance and Reconnaissance (ISR), and capturing high resolution pictures of a moving ground target with different speeds. The need to capture a moving target especially at low speeds demands the UAVs capability to maintain equilibrium flight at the intended speed and at high angles of attack (in some cases) during flight. To fulfil the needs of multipurpose missions, a wide-ranging variety of UAVs, with different sizes and performances, have been designed and built.

One of the classifications of UAVs is the Micro Air Vehicle (MAV). By definition, MAVs are defined by

dimensional restriction of 6 inches in its length, width and height [2] with takeoff weight of approximately 200g. MAVs are significantly smaller in size and are designed to maneuver in tight or constrained environment at low speed to capture good quality visual information [3]. The regime where MAVs are restricted to fly is low Reynolds number regime (~0.15 Million) which is also known for its flow-field complexity. Several complex phenomena like laminar flow separation, transition and reattachment occur within the boundary layer of its small surface in this regime. Moreover, the lift-to-drag ratio is drastically reduced at low Reynolds number thereby aggravating the problem of aerodynamic efficiency. There might not be sufficient lift to carry its payload, therefore become unsuitable for field operations. Different configurations such as convertible platforms [4, 5], flapping wing [6], flexible wing [7], quadrotors [8] and other versatile concepts [9-11] are explored. One of the solutions to produce additional lift is the usage of a second wing on board [12-15] commonly known as biplane configuration.

Biplane configuration has generally three geometric parameters namely gap between the wings, stagger and decalage angle. Stagger is the position of the upper wing with respect to the lower wing. Decalage angle is the angle of the upper wing with reference to the lower wing. Stagger and decalage angle generally contribute less in the whole configuration so taking these parameters as constant; the only variable geometric parameter is the gap between the wings [13, 16].

Traub [17] evaluated the possibility of biplane delta wing configuration as an aerodynamically efficient platform for MAV applications. Delta wings with 75 deg of sweep are used during investigations. Polhamus [18] leading edge suction analogy and Prandtl lifting theory are combined to develop theoretical estimation technique. It is observed that stagger effects are less pronounced than gap. Although experimental validation is carried out for the theoretical model, however, the applicability of the theoretical model with other planform shapes such as elliptical, rectangular, Zimmerman or inverse Zimmerman is yet to be seen. Similarly, Moschetta and Thipyopas [14] compared the performance of monoplane MAV with a biplane configuration. The study encompasses the

Manuscript received May 6, 2018; revised August 7, 2018.

optimization of geometric variables (stagger, gap, decalage angle and aspect ratio) through numerical and wind-tunnel investigations. The propeller interaction with the biplane configuration is also studied. The observations report the promising potential for biplane MAVs as an alternative to monoplane platforms such as Black Widow MAV (monoplane).

This research article is based on the flight performance and longitudinal stability of biplane MAVs under the effect of geometric variable gap between two wings. The study is conducted for three planform shapes; Zimmerman, inverse Zimmerman and elliptical; and aspect ratio one. Stagger and decalage angle contribute less in the whole configuration so taking these parameters as constant, the only variable geometric parameter is the gap between the wings. The focus is to assess the effect of gap, if any, on the flight performance and stability characteristics in longitudinal plane.

II. AERODYNAMIC DATA MODELING

The aircraft planform, considered here, has typical dimensional attributes that include mass of 56.5 g [19] and additional mass of 10 g for the second wing of the biplane configuration. The wing planform shapes are elliptical, Zimmerman and inverse Zimmerman with aspect ratio of one and chord length of 0.172491 m as shown in Fig.1. Wing area for monoplane configuration is 0.0127 m². For biplane configuration, two wings of chord length 0.172 m and wing area of 0.0255 m² with gap values of 0.289c̄ (5cm) , 0.696c̄ (12cm) , 0.928c̄ (16cm) and 1.160c̄ (20cm) are considered. The stagger and decalage angle are set at zero and considered constant in this study.

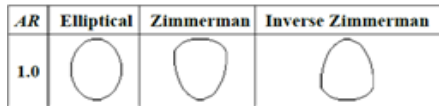


Figure 1. Wing models used in wind tunnel experiments

The wind tunnel experiments for both monoplane and biplane configurations are conducted at Nanyang Technological University, Singapore in a low-turbulence open-circuit wind-tunnel. The wind speed of the wind tunnel ranges from 3 to 21 m/s. The test section used is 2 m long with rectangular cross-section area of 1 by 1 m. Data collection is made by a load cell mounted on a sting support where the wing model is attached. The sting support is capable of generating angles of attack in the range of ±30 deg. The aerodynamic coefficients presented in this work, are corrected for wind-tunnel blockage effects according to the techniques presented by Barlow *et al.* [20]. No hysteresis is recorded in the readings. Monoplane results are validated with data of Torres and Mueller [21].

Generally, MAV flies approximately between 117000 and 157000 Reynolds Number regime depending on the wing. So to give representation value of MAV flight velocities, all wind tunnel runs were conducted at an air speed of 12 m/s. During data collection, it is assumed that the lift, drag and moment can be considered independent of the small variation in Reynolds Number for all wings

used. For instance, the data for Zimmerman planform configuration is tabulated in Table I.

TABLE I. AERODYNAMIC PARAMETERS FOR MONOPLANE AND BIPLANE ZIMMERMAN PLANFORM CONFIGURATION

Configuration	Monoplane (cm)	Biplane Gap			
		5cm	12cm	16cm	20cm
S (m)	0.025	0.051	0.051	0.051	0.051
W (N)	0.057	0.066	0.066	0.066	0.066
<i>k</i>	0.335	0.335	0.335	0.335	0.335
<i>C_{Lmax}</i>	0.966	0.479	0.799	0.859	0.863
<i>C_{D0}</i>	0.049	0.037	0.036	0.033	0.033
(<i>L/D</i>) _{max}	3.891	4.519	4.541	4.761	4.732

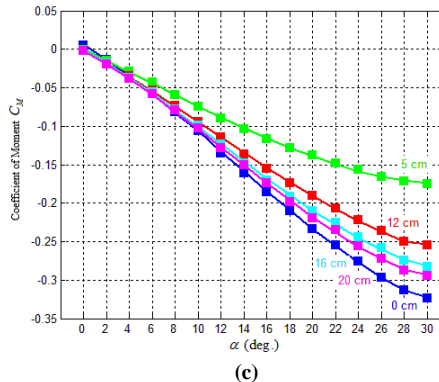
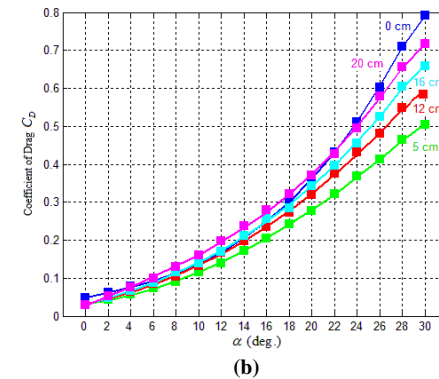
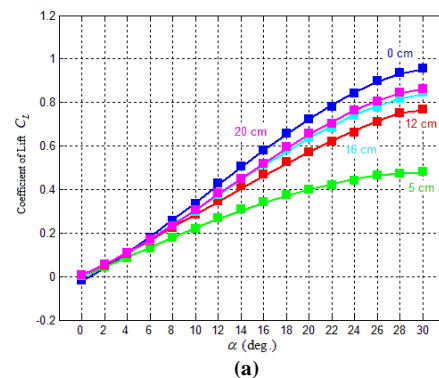


Figure 2. Coefficient of lift, (b) coefficient of drag and (c) coefficient of moment of Zimmerman planform-AR=1 for monoplane and biplane with gap variations

The lift, drag and moment coefficients obtained through wind-tunnel testing across angle of attack ranging from

0° to 30° under gap variation for elliptical, Zimmerman and inverse Zimmerman planforms are plotted in Fig. 2. For post-stall data estimation, a technique proposed by Viterna and Corrigan [22, 23] is used. The model is based on fitting the curve to angle of attack α greater than stall but less than 90°. The formulation is given as:

$$C_L = A_1 \sin 2\alpha + A_2 \frac{\cos^2 \alpha}{\sin \alpha} \quad (1)$$

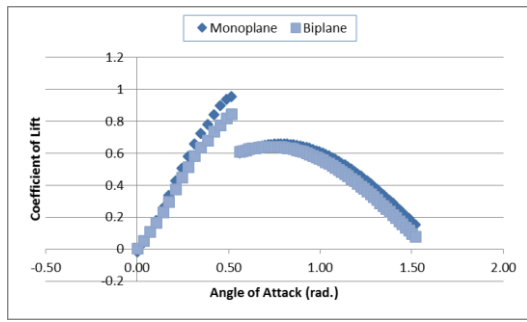
$$C_D = B_1 \sin^2 \alpha + B_2 \sin \alpha$$

where,

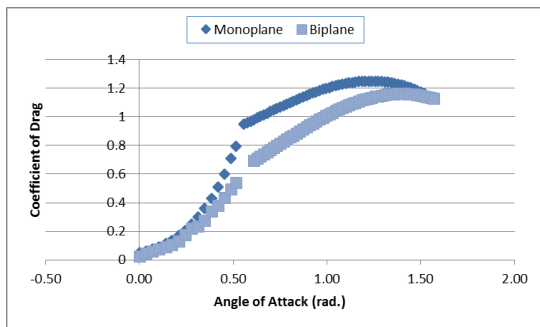
$$A_1 = \frac{B_1}{2}, \quad A_2 = \left(C_{L, stall} \frac{\sin \alpha_{stall}}{\cos^2 \alpha_{stall}} - C_{D, max} \sin \alpha_{stall} \cos \alpha_{stall} \frac{\sin \alpha_{stall}}{\cos^2 \alpha_{stall}} \right)$$

$$B_1 = C_{D, max}, \quad B_2 = \frac{C_{D, stall} - C_{D, max} \sin^2 \alpha_{stall}}{\cos \alpha_{stall}}$$

The resultant post-stall data of aerodynamic forces from 30 to 90 degrees is plotted in Fig. 3. The $C_{D, max}$ is the maximum coefficient of drag and can be calculated using aspect ratio AR as follows:



(a)



(b)

Figure 3. Post-stall approximation of (a) coefficient of lift, (b) coefficient of drag for monoplane and biplane configurations

$$C_{D, max} = 1.1 + 0.018AR \quad (2)$$

III. FLIGHT PERFORMANCE ESTIMATION

The flight performance of both monoplane and biplane under gap variations is compared and discussed. The configuration which is used for both monoplane and biplane will be identical to the wings, used for the wind tunnel testing. Equation (3) states that maximum lift to drag ratio is dependent on the reciprocal of the zero lift drag C_{D_0} , and the induced drag coefficient k , as the

increase in both factors will result in reducing the ratio and vice versa. The induced drag coefficient k for both monoplane and biplane is taken to be 0.335. The zero lift drag C_{D_0} of monoplane is comparatively higher than all biplane cases, so the ratio is ultimately reduced. Within gap variations, $(L/D)_{max}$ ratio increases as the gap is increased as shown in Table I.

$$\left(\frac{L}{D} \right)_{max} = \frac{1}{\sqrt{4kC_{D_0}}} \quad (3)$$

Equation (4) shows minimum thrust required that depends on the weight of the aircraft W , zero lift drag C_{D_0} , and the induced drag coefficient k . It can be observed that gap variation has insignificant effect on minimum thrust requirements. The only difference between monoplane and biplane weight is the difference of the single wing, that is 10 g. Also, the effect of planform shape has negligible effect on minimum thrust requirement as shown in Fig. 4.

$$T_{R, min} = 2W \sqrt{kC_{D_0}} \quad (4)$$

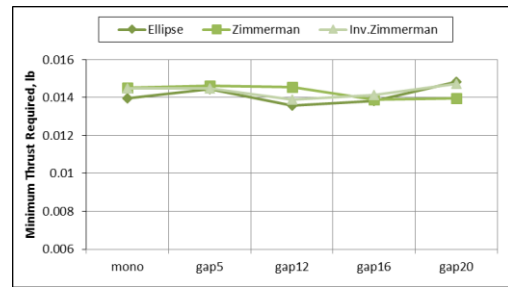


Figure 4. Minimum thrust required for monoplane and biplane configurations under gap variation for different planform shapes

Equation (5) shows minimum power required for flight. It can be observed that monoplane requires more power to move forward because of higher value of C_{D_0} than biplane. As velocity increases, the induced drag will increase and dominate the total drag. For biplanes, the effect of gap and planform shape does not govern the minimum power requirements as can be observed in Fig. 5.

$$P_{R, min} = \sqrt{\frac{2W^3}{\rho S} \left(\frac{C_D^2}{C_L^3} \right)_{min}} \quad (5)$$

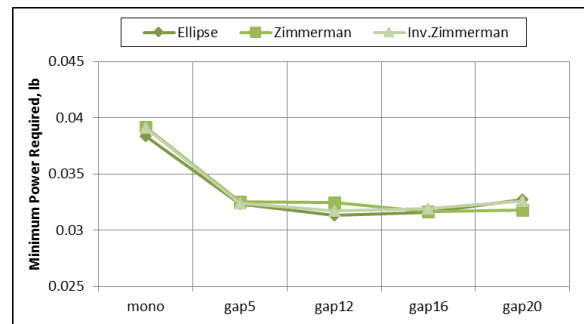


Figure 5. Minimum power required for monoplane and biplane configurations under gap variation for different planform shapes

Equation (6) represents velocity of aircraft at minimum power required and corresponding effect on monoplane and biplanes. The results are consistent with minimum power requirements behavior (see Fig. 6).

$$V_{P_{min}} = \sqrt{\frac{2W}{\rho S} \sqrt{\frac{k}{3C_{D_0}}}} \quad (6)$$

Equation (7) represents the stall speed majorly contributed by wing loading W/S and maximum coefficient of lift $C_{L_{max}}$. In biplane case, the wing loading is lower than monoplane due to its increase in wing area. However, for biplane, is lower than monoplane because there is flow interference between the wings. As the gap between the wings increases in biplane case, value varies the stall speed.

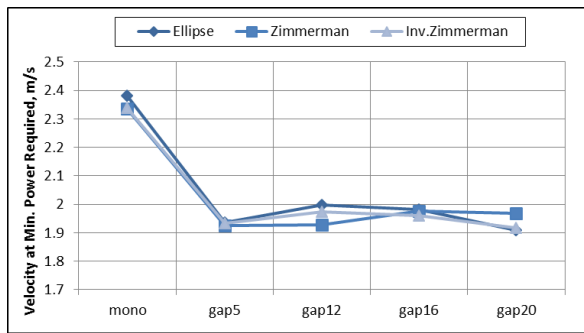


Figure 6. Velocity at minimum power required for monoplane and biplane configurations under gap variation for different planform shapes.

Monoplane has lower stall speed than the biplane with smaller gap, but as the gap increases the stall speed reduces, thus biplane performs better for surveillance missions (see Fig. 7).

$$V_{stall} = \sqrt{\frac{2W}{\rho S} \frac{1}{C_{L_{max}}}} \quad (7)$$

$$\tan \gamma_{g_{min}} = \frac{1}{(L/D)_{max}} \quad (8)$$

Equation (8) represents the angle achieved by an aircraft at unpowered flight mode i.e. in gliding mode. Minimum glide angle is inversely proportion to maximum lift to drag ratio. The biplane will have a relatively smaller glide angle than monoplane, because

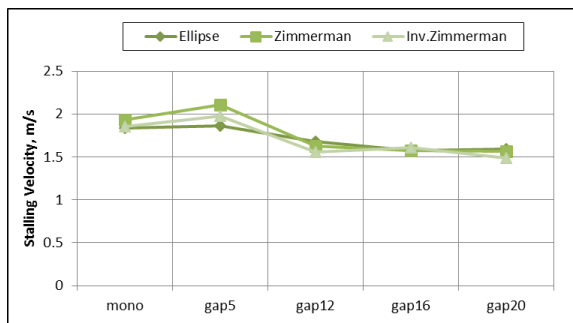


Figure 7. Stall speed for monoplane and biplane configurations under gap variation for different planform shapes

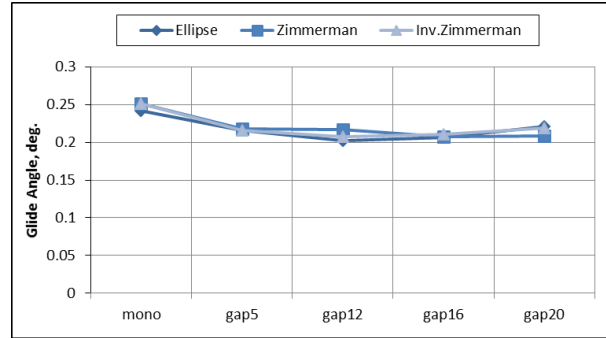


Figure 8. Gliding Angle for monoplane and biplane configurations under gap variation for different planform shapes.

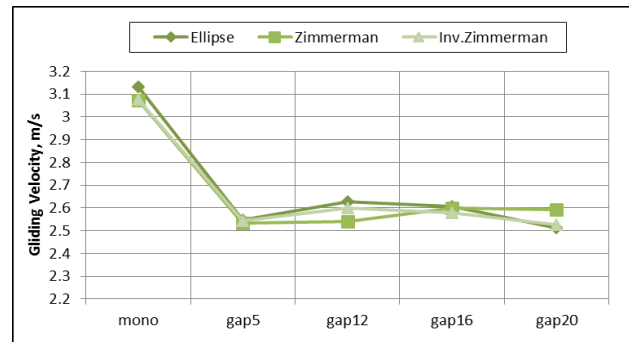


Figure 9. Gliding velocity for monoplane and biplane configurations under gap variation for different planform shapes

$(L/D)_{max}$ is high in monoplane configuration (see Fig. 8).

$$V_{glide} = V_{(L/D)_{max}} = \sqrt{\frac{2W}{\rho S} \sqrt{\frac{k}{C_{D_0}}}} \quad (9)$$

However, the effect of gap and planform shape on minimum glide angle is indistinguishable and in equation (9) velocity in gliding mode is presented. This velocity is dependent on the wing loading and parameters of drag coefficient. It is higher in the case of monoplane configuration, and gets lower for all the gaps in biplane configuration. The lower velocity in biplane configuration makes it ideal that it can also fly when in the gliding mode (see Fig. 9).

Endurance is meant by the actual time of flight in minutes. Equation (10) is expressed in the reciprocal of the power required. The efficiency factor ϵ_A and load factor n of 0.95 and 1.0 are assumed respectively [13]. As a guide, the propulsion system and battery source of the Black Widow are assumed to be used by monoplane and biplane configurations. This parameter tells that how long an aircraft has its flight when the aircraft is battery powered and the results are plotted (see Fig. 10).

$$E = \frac{n\epsilon_A}{P_R} \quad (10)$$

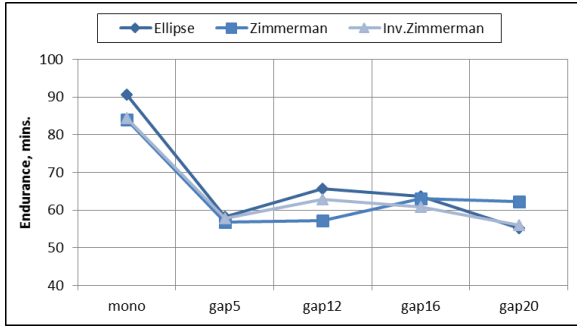


Figure 10. Endurance for monoplane and biplane configurations under gap variation for different planform shapes

Equation (11) represents that how far an aircraft can go from the remote station and it depends on the endurance calculated. Since the propulsion system for monoplane and biplane is same and biplane has added weight, therefore, the range of biplane is less than monoplane (see Fig. 11).

$$R_g = \int_0^E V_g dt \quad (11)$$

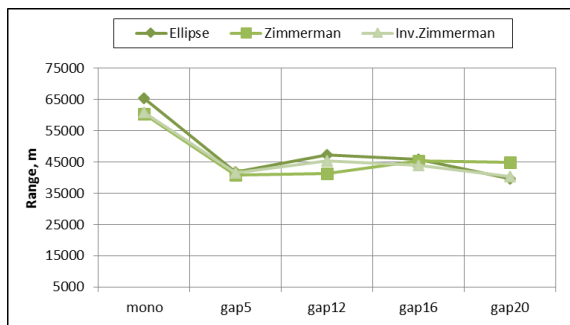


Figure 11. Range for monoplane and biplane configurations under gap variation for different planform shapes

It can be concluded from Figures 4 to 11 that the effect of gap is insignificant in the evaluation of flight performance for different planform shapes. However, typical studies only focus on the aerodynamic performance thereby unable to generate complete picture on flight performance characteristics. So, for trim analysis and longitudinal stability evaluation of biplane configuration, a higher gap i.e., $0.928\bar{c}$ (16cm) is used.

IV. TRIM ANALYSIS

Both monoplanes and biplanes are symmetric about their vertical axis. This enables their longitudinal dynamics to be decoupled. The equations stated below represent the longitudinal motion of the aircraft along the body axes. These equations are non-linear and a simple procedure using small perturbation theory is required to linearize them about a specific trim point. [24]

$$\dot{u} = X/m - g \sin \theta - qw \quad (12)$$

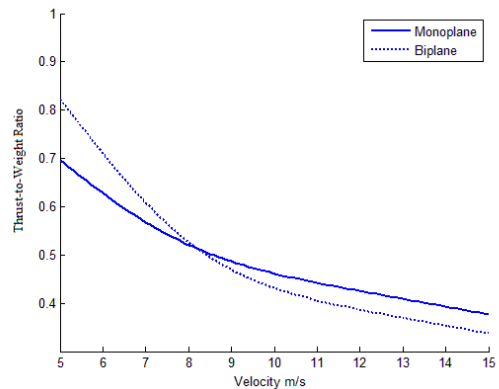
$$\dot{w} = Z/m + g \cos \theta + qu \quad (13)$$

$$\dot{q} = M/I_{yy} \quad (14)$$

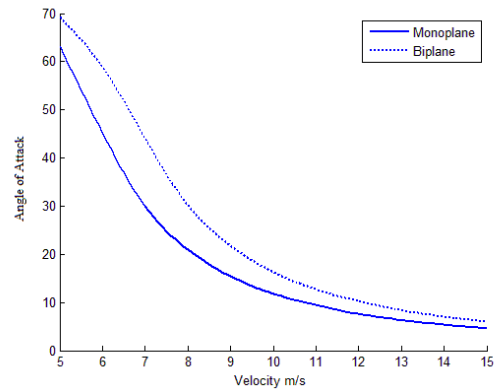
$$\dot{\theta} = q \quad (15)$$

X and Z represent the horizontal and vertical force vectors; u and w show the horizontal and vertical velocities; M is the pitching moment; g is the acceleration due to gravity; q is the pitch rate; m is the mass of the aircraft and I_{yy} is the moment of inertia in the longitudinal mode [24].

Analysis of steady-state trimmed flight conditions is carried out at various airspeeds. In order to obtain the trim flight conditions, a numerical approach is used. The problem is expressed as a nonlinear constrained optimization problem and to find the trimmed flight conditions, *fmincon*, the MATLAB® routine, is used [25, 26]. Velocity range varying from 5 to 15 m/s is considered for trim analysis.



(a)



(b)

Figure 12. Control requirements to trim the UAVs: (a) Thrust to Weight ratio and (b) angle of attack for monoplane and biplane Zimmerman planform

The motion has two degrees of freedom of translational dynamics. Thrust and angle of attack are taken as control variables.

$$\vec{c} = [\alpha; T/W]^T \quad (16)$$

The cost function to be minimized in the optimization is as follows:

$$F = X^2 + Z^2 \quad (17)$$

where X and Z are the components of the resultant forces. The constraints posed to the state variables are:

$$\begin{cases} 0^{\circ} \leq \alpha \leq 90^{\circ} \\ 0 \leq T/W \leq 1.00 \end{cases} \quad (18)$$

From several initial guesses, single trim states, across different velocities, are evaluated for monoplane and biplane cases as shown in Fig. 12. It is concluded that the thrust-to-weight ratio for monoplane is lower than biplane at velocity of 5 m/s. Biplane requires higher thrust-to-weight ratio because it is slightly heavier in weight than monoplane so at lower velocities, it requires more thrust to hold altitude. After the break-even point of 8-9 m/s, biplanes come in pre-stall regime and thus aerodynamic forces start to play more dominant role, thereby suppressing the requirement of high thrust-to-weight ratio.

V. NUMERICAL SIMULATIONS

In this section, the longitudinal dynamics of aircraft models under study is simulated using standard nonlinear coupled equations of motion. The focus of the simulations is to capture the qualitative differences between monoplane and biplane dynamic responses,

$$\dot{V} = \frac{1}{m} [T \cos(\alpha + i) - D - mg \sin \gamma] \quad (19)$$

$$\dot{\gamma} = \frac{1}{mV} [T \sin(\alpha + i) + L - mg \cos \gamma] \quad (20)$$

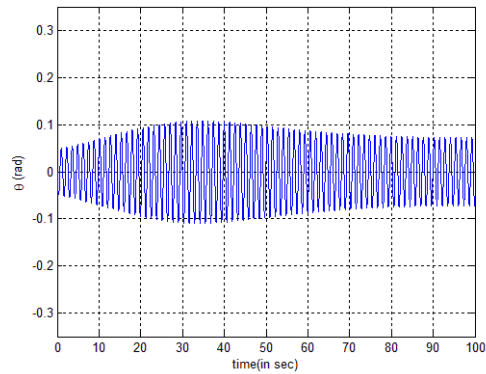
$$\dot{q} = M / I_{yy} \quad (21)$$

$$\dot{\alpha} = \dot{\theta} - \dot{\gamma} = q - \frac{1}{mV} [T \sin(\alpha + i) + L - mg \cos \gamma] \quad (22)$$

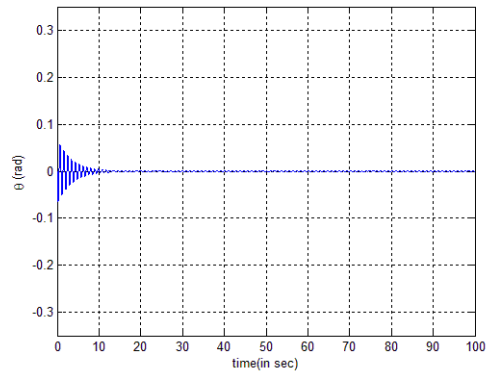
where V is the velocity; γ is the flight path angle; i is the wing incidence angle and I_{yy} is the moment of inertia in the longitudinal mode. For the numerical simulations, *ode45*, a built-in function in MATLAB[®]'s differential equation solver, based on classical fourth-order Runge–Kutta method, is used to incorporate the nonlinear longitudinal equations of motion [27]. The details of trim conditions, angle of attack and thrust, for the velocities varying from 4-7 m/s for both monoplane and biplane configurations are as follows:

TABLE II. THRUST AND ANGLE OF ATTACK AT VARIOUS VELOCITIES

	Velocity (m/s)	Thrust (N)	Angle of attack (rad)
Monoplane	4	0.684	1.103
	5	0.576	0.788
	6	0.488	0.521
	7	0.435	0.367
Biplane	4	0.861	1.237
	5	0.783	1.028
	6	0.658	0.769
	7	0.544	0.527



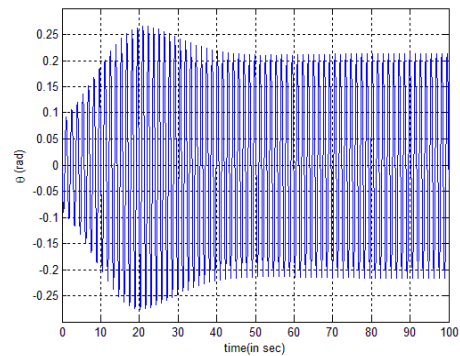
(a)



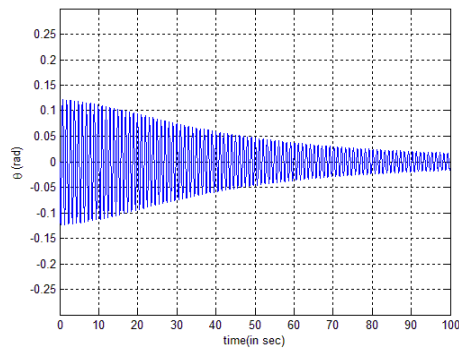
(b)

Figure 13. Response of pitch angle for monoplane case for the velocities (a) 4 m/s, (b) 5 m/s

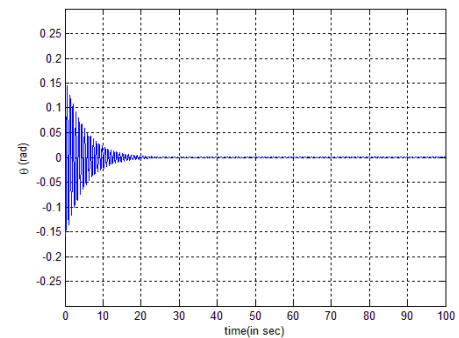
In Fig. 13, response of the pitch angle for the monoplane configuration is illustrated. For velocity of 4 m/s, limit cycles oscillations are generated. Initially small magnitude oscillations are generated that grow as time increases, but after 35 seconds, oscillation decay and shows almost a constant behavior later on. For velocity of 5 m/s, initial oscillation is higher in magnitude and then stabilizes after 20 seconds. Similar behavior of stability is observed for velocities 6 m/s and 7 m/s, where the configuration shows stable behavior. As far as angle of attack is concerned, similar behavior is observed for velocity 4 m/s and 5 m/s as it is shown in pitching angle, this is because the angle of attack is a function of pitch angle and flight path angle.



(a)



(b)

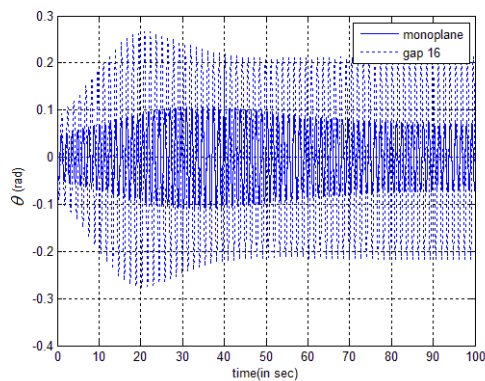


(c)

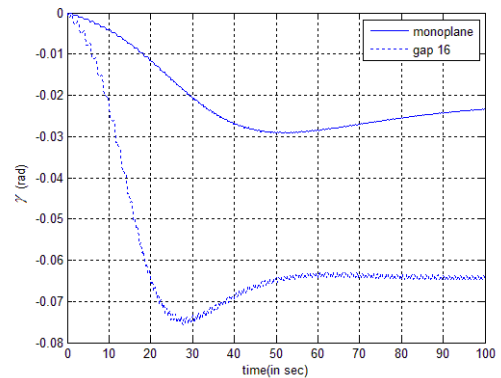
Figure 14. Response of pitch angle for biplane case for the velocities (a) 4 m/s, (b) 5 m/s and (c) 6 m/s

For biplane configuration the response of the pitch angle is plotted in Fig. 14. The limit cycle oscillations are generated in higher magnitude in biplane configuration as compared to monoplane configuration for 4 m/s velocity. Later on, as velocity increases, this configuration converges to stability but it takes much more time than monoplane configuration. This behavior continues for the velocities 6 m/s and 7 m/s, where the configuration turns stable after 30 seconds and 10 seconds respectively. It is observed here that angle of attack is behaving similar to pitching angle but with slight increase in amplitude.

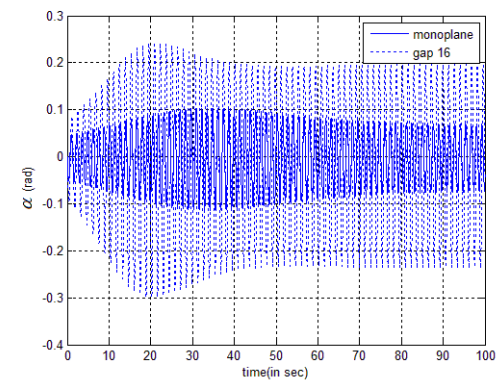
Pitch angle, flight path angle and angle of attack are compared for monoplane and selected biplane configurations for the velocity of 4 m/s and illustrated in Fig. 15. This comparison shows that the amplitude of limit cycle oscillations for biplanes is much larger than monoplanes.



(a)



(b)



(c)

Figure 15. Comparison of numerical simulation of (a) pitch angle, (b) flight path angle and (c) angle of attack for monoplane and biplane 4 m/s.

VI. CONCLUSION

From performance analysis, it is concluded that maximum lift to drag ratio and minimum power required for biplane is better than for monoplane configuration. From trim studies it is observed that at lower velocities, biplane configuration is much superior to monoplane configuration but as velocity increases, this behavior reverses and monoplane performs better. Moreover, biplane tends to go in Limit Cycles Oscillations earlier than monoplane configuration which makes it unsuitable for flying at higher velocities. Hence, at lower velocities biplanes are superior to monoplanes; however they are not recommended for a flight at higher velocities. The amplitude of biplane configuration is higher therefore LCO suppression control system needs to be developed in order to mitigate the deleterious consequences of LCO. Gap variation for different planform shapes does not seem to have a significant effect in overall analysis.

ACKNOWLEDGEMENT

The authors would like to acknowledge Dr. Tiauw Hiong Go for helping in generating aerodynamic data related to this work. The work was supported by National University of Sciences & Technology and the numerical part was run on the HPC at the Research Centre for Modeling & Simulation

REFERENCES

- [1] R. M. Rais and H. G. R., "Multidisciplinary design and prototype development of a micro air vehicle," *Journal of Aircraft*, p. 36, 1999.
- [2] R. C. Michelson, "Novel approaches to miniature flight Platforms," in *Proc. the Institution of Mechanical Engineers. Journal of Aerospace Engineering*, p. 218, 2004.
- [3] C. Thipyopas and M. J. M., "From development of micro air vehicle testing research to the prototype of TYTO, low speed biplane MAV," in *Proc. 26th AIAA Applied Aerodynamics Conference*, Honolulu, HI, United states., 2008.
- [4] A. Maqsood, Go, and T. H., "Optimization of hover-to-cruise transition maneuver using variable-incidence wing," *J. Aircr.*, vol. 47, no. 3, pp. 1060–1064, 2010.
- [5] A. Maqsood and T. H. Go, "Design improvement of a versatile ducted-fan UAV," *Journal of Mechanical Engineering*, vol. 9, pp. 1-17, 2012.
- [6] R. Ramamurti and W. Sandberg, "Computation of aerodynamics characteristics of a micro air vehicle," in *Fixed and Flapping Wing Aerodynamics for Micro Air Vehicle Applications*, *American Institute of Aeronautics and Astronautics*, vol. 195, 2001.
- [7] A. Maqsood and H. G. Tiauw, "Aerodynamic characteristics of a flexible membrane micro air vehicle," *International Journal of Aircraft Engineering and Aerospace Technology*, vol. 87, pp. 30-37, 2015.
- [8] T. Deif, A. Kassem, and G. El Baioumi, "Modeling and attitude stabilization of indoor quad rotor," *International Review of Aerospace Engineering*, vol. 7, pp. 43-47, 2014.
- [9] M. Manzoor, A. Maqsood, and A. Hasan, "Quadratic optimal control of aerodynamic vectored UAV at high angle of attack," *International Review of Aerospace Engineering* vol. 9, pp. 70-79, 2016.
- [10] M. A. Aziz and A. Elsayed, "CFD Investigations for UAV and MAV low speed airfoils characteristics," *International Review of Aerospace Engineering*, vol. 8, pp. 95-100, 2015.
- [11] D. J. P. A. F. Bohoquez, "Challenges facing future micro-air-vehicle development," *Journal of Aircraft* vol. 43, ed, 2006, pp. 290-305.
- [12] H. Kang, N. Genco, and A. Altman, "Empirically derived biplane lift as a function of gap and stagger," *Journal of Aircraft*, vol. 50, January-February 2013 2013.
- [13] A. Maqsood, Go, and T. H., "Parametric studies and performance analysis of a biplane micro air vehicle," *International Journal of Aeronautical and Space Sciences*, vol. 14, pp. 229-236, 2013.
- [14] J. M. Moschetta and C. Thipyopas, "Aerodynamic performance of a biplane micro air vehicle," *Journal of Aircraft*, vol. 44, pp. 291-299, 2007.
- [15] I. R. L. Roedts, "Design of a biplane wing for small-scale aircraft," presented at the *47th AIAA Aerospace Sciences Meeting including the New Horizons Forum and Aerospace Exposition*, Orlando, FL, United states, 2009.
- [16] A. Maqsood, T. C. C. Wei, and T. H. Go, "Experimental investigation of a Bi-plane micro air vehicle," presented at the 28th International Congress of the Aeronautical Sciences, 2012.
- [17] L. W. Traub, "Theoretical and experimental investigation of biplane delta wings," *Journal of Aircraft*, vol. 38, 2001.
- [18] E. C. Polhamus, "A concept of the vortex lift of sharp-edge delta wings based on a leading-edge-suction analogy," 1966.
- [19] J. M. G. A. M. T. Keennon, "Development of the black widow micro air vehicle," in *Aerospace Sciences Meeting and Exhibit, Reno, NV*, 2001.
- [20] J. B. Barlow, *Low-Speed Wind Tunnel Testing*, 3 ed.: Wiley, 1999.
- [21] G. E. Torres and T. J. Mueller, "Low-aspect-ratio wing aerodynamics at low reynolds numbers," *AIAA Journal*, vol. 42, pp. 865-873, 2004.
- [22] L. A. Viterna and D. C. Janetzke, "Theoretical and Experimental Power from Large Horizontal-axis Wind Turbines.," Technical Report TM-829441982.
- [23] L. A. Viterna and R. D. Corrigan, "Fixed pitch rotor performance of large horizontal axis wind turbines," in *DOENASA Workshop on Large Horizontal Axis Wind Turbines*, Cleveland, Ohio, 1981.
- [24] A. Maqsood and T. H. Go, "Longitudinal flight dynamic analysis of an agile UAV," *Aircraft Engineering and Aerospace Technology*, vol. 82, pp. 288-295, 2010.
- [25] A. Maqsood and T. H. Go, "Optimization of hover-to-cruise maneuvers for an agile unmanned aerial vehicle using variable-incidence wing," *Journal of Aircraft*, 2010.
- [26] A. Maqsood and G. Tiauw Hiong, "Optimization of transition maneuvers through aerodynamic vectoring," *Aerospace Science and Technology*, vol. 23, pp. 363-371, 2012.
- [27] A. Maqsood and G. T. Hiong, "Multiple time scale analysis of aircraft longitudinal dynamics with aerodynamic vectoring," *Nonlinear Dynamics*, vol. 69, pp. 731-742, 2012.



Muhammad Usman received his BS-Mathematics degree from COMSATS Institute of Information Technology, Islamabad, Pakistan, in 2012 and MS in Computational Science and Engineering (CS&E) from Research Center for Modeling and Simulation (RCMS), National University of Sciences and Technology (NUST), Islamabad, Pakistan in 2015. Currently, he is a doctoral candidate at Xian Jiaotong University, China. His research interests are associated with mathematical modeling and simulation, fluid dynamics and engineering dynamics.



Dr. Adnan Maqsood is working as Assistant Professor at National University of Sciences and Technology (NUST), Pakistan, since 2012. He received his Bachelor's degree in Aerospace Engineering from NUST, Pakistan in 2005 and PhD from Nanyang Technological University (NTU), Singapore in 2012. Currently, he is engaged in graduate teaching and research at Research Centre for Modeling & Simulation and heading Mechanics Interdisciplinary Group (MIG) that work in the broad areas of Aerodynamics, Flight Mechanics & Control (AFMC). He has done significant research work and published several top quality international conferences and journal papers. He has been often invited as a reviewer for a number of conferences, journals and book reviews. His current research interests are associated with Applied & Computational Aerodynamics, Flight Dynamics and Control, Unmanned Air Vehicle (UAV) Systems, Nonlinear Dynamics and Wind Energy.



Sundas Rafat Mulkana is currently working as a Research Assistant at Research Centre for Modeling and Simulation, NUST. She has received a bachelor's degree in Aerospace Engineering in 2015 and is pursuing Masters in Systems Engineering. Her research interests span across System Architecture and Design, Space Systems, Health Systems, Multidisciplinary Design Optimization and

Micro Aerial Vehicles.



Dr. Rizwan Riaz is working as Professor and Dean at Research Centre for Modeling & Simulation, National University of Sciences and Technology (NUST), Pakistan. He received his Bachelor's in Aeronautical Engineering from United States Air Force Academy (USAF), USA in 1990, Masters in Aerospace Engineering from NUST, Pakistan in 2004 and PhD in Mechanical Engineering (CFD-Aeroacoustics) from University of Manchester, UK, in 2008. Currently, he is engaged in graduate teaching and research at Research Centre for Modeling & Simulation. He holds industrial experience of more than two decades. His current research interests are associated with Computational Fluid Dynamics, Aeroacoustics, Turbomachinery and Aircraft Design.